Complex group lasso and adaptive complex group lasso for sparse damage detection

V. Dimopoulos [1,2]**, E. Deckers** [2,3]
[1] KU Leuven, Department of Mechanical Engineering,
Celestijnenlaan 300, B-3001, Heverlee, Belgium
e-mail: **vasileios.dimopoulos@kuleuven.be**

[2] DMMS Core lab, Flanders Make, Belgium

[3] KU Leuven, Campus Diepenbeek, Department of Mechanical Engineering,
Wetenschapspark 27, B-3590 Diepenbeek, Belgium

Abstract
Identifying the location of damage in civil and mechanical structures has been the focus of engineers for many years. In particular, sparsity-based algorithms have recently gained traction as robust and cost-effective techniques for inspection with limited information. In this paper, we present a sparsity-enabled damage localization method that operates with a single sensor observing low-frequency structural responses. The obtained information, in the form of transfer functions, is processed with a Group Lasso minimization routine. The algorithm relies on an $L_{2,1}$-norm penalty that is able to promote sparsity while also treating complex frequency responses. In addition, an adaptive variation of the routine is introduced that further enhances detectability. Both techniques are experimentally validated on a composite plate with artificially and permanently induced defects. Damage maps of high resolution and detectability are obtained. A comparison with a full-array super-resolution algorithm shows that both methods are of high and competitive performance.

1 Introduction

Mechanical structures are often exposed to hostile environmental conditions while also having to withstand varying loading. Such a combination of uncertainty elements leads to the gradual or even abrupt structural degradation. Although the latter may significantly compromise the structural integrity, the earlier stages of damage development tend to occur as a localized phenomenon which only if neglected will evolve into a threat. Early damage detection and localization are hence a critical element to satisfy safe and efficient operations. A number of methods have been proposed to this end. In particular, a large number of them manages to localize degradation by investigating changes on the modal characteristics of the structure once damage occurs [1, 2, 3]. Another approach analyzes wave propagation in the structure searching for potential wave-damage interactions [4, 5, 6]. These methods are able to extract information about the defect's location and severity. In any case, to perform structural inspection, the system's responses must be first acquired. To measure such responses researchers use dedicated aperture able to resolve the vibrating structure's displacement, velocity or acceleration [7, 8, 9]. Nevertheless, a common limitation for the structural inspection is the need for large numbers of these measurements. Of course such a time-consuming process has direct and cost-related impact on the structure's operation. A secondary limitation of the extensive measuring campaign is the inaccessibility of certain locations on the structure. This has as a result for some parts of the geometry to be impossible to get directly inspected.

Compressive sensing tries to answer these problems by introducing techniques able to localize damage with a small number of measurements. These methods aim to reconstruct damage related information starting from partial knowledge for the problem at hand. A common approach to reconstruct the missing information is by

assuming some knowledge for the fundamental properties of the solution. In the case of damage detection such a property can be the sparsity of the problem. A sparse solution for the inspection process is a solution that returns a small number of defects. Such an assumption is quite reasonable for the early stages of damage evolution considering it is often a rare and local phenomenon. This assumption serves as a much needed constraint for the process of identifying damage with a small number of measurements.

Dedicated algorithms have been proposed to solve sparsity-constraint problems. Ridge regression is a first attempt to this end. This algorithm solves a linear minimization problem by means of a penalized Ordinary Least Squares problem (OLS) [10] The penalty has the form of the L_2-norm of the solution so that the recovered approximation is sparse in the exploration space. Tibshirani [11] proposed the Lasso algorithm and achieved higher levels of sparsity by substituting the L_2-norm of Ridge regression with a L_1-norm penalty. L_1-norms naturally serve as a convex approximation of the L_0-norm while promoting sparsity. Modifications have been proposed for the Lasso algorithm to enhance its performance and introduce structure in the solution. For the prior, Zou [12] proposed the adaptive Lasso that enhances resolution and enables the oracle property throughout the regularization path. Furthermore, Yuan [13] introduced structure in the solution with the Group Lasso algorithm. This technique allows variables in the solution vector to be separated in non-overlapping groups. The algorithm introduces then a $L_{2,1}$-norm to enforce the j^{th} variable in each of the groups to be simultaneously selected or excluded from the model.

Smith et al. [14] utilized sparsity for damage localization on a sensitivity-based framework. In their work, they demonstrated that small changes happening on an impulse responses between the reference and the damaged states can be approximated as a linear combinations of sensitivity vectors. These vectors are a function of the stiffness and they can be obtained with respect to the structure's modal parameters. The linear approximation defines then a regression problem which if solved with the Lasso algorithm resolves damage locations. Zhou et al. [15] applied the sensitivity method to localize damage in beam structures using low-frequencies modal information. Entezami et al. [16] enhanced the performance of the sensitivity method by proposing an improved sensitivity function of the modal strain energy. With a different approach, Sen et al. [17] defined a number of possible damage locations and measured the scattered responses occurring in each case when placing the damage there. Any subsequent scattered signals during inspection can then be decomposed with the basis of simulated responses. This time-domain technique was seen able to localize defects. Yang et al. [18] localized damage after blindly extracting modal feature vectors for the construction of the decomposition basis. Xu [19] used sparse regression to extract Time-Of-Flight information for the propagating waves. This information was then introduced in a DAS [20] algorithm to localize the defects. Mesnil et al. [21] managed to reconstruct the wavefield of a damaged structure using a sparse approximation based on dispersion information of the medium. The reconstructed field is able to recover both the excitation and a defect installed on the system.

In this paper a Group Lasso method is presented which manages to localize defects by grouping real and imaginary components from a basis composed of transfer functions. Then the sparsity constraint is applied to localize damage. Grouping the variables allows for complex-valued frequency domain responses to be easily processed. An adaptive variation is also seen to localize damage with higher accuracy for multiple defects and noisy environments. Section 2 establishes the analytic basis for the sparse approximation of the damage-emitted information. Section 3 introduces the sparsity-enabled methods for the damage detection. Section 4 presents a series of experiments performed to validate the proposed techniques while section 5 discusses the results. Section 6 concludes the paper.

2 The signal model for damage localization

In this section, the signal model that enables the damage localization is introduced. Specifically, focusing on the wavefields emitted due to the presence of defects in the structure, an approximation is made that allows those signals to be decomposed in terms of the transfer functions of the background medium. This approximation reveals strong dependencies between the received wavefields and the transfer functions corresponding to locations of damage. As a result a damage map can be produced that highlights the identified defect zones.

2.1 Scattered field approximation

Consider wave propagation in an elastic medium with a single embedded point-scatterer. The resulting wavefield arises as the superposition of healthy medium propagation and waves emitted from the defect. Assuming linear propagation, the latter is isolated as the difference in the responses between the healthy and the damaged state. The obtained waves comprise the scattered field. Assuming that an impact was used for the excitation, the scattered field can be expressed in the frequency domain with the use of transfer functions for the system. Specifically, in Equation (1), the scattered information on the left-hand side is expressed as a three-term multiplication on the right-hand side:

$$sc(f) = t_E(f) * d(f) * t_S(f). \tag{1}$$

The first term $t_E(f)$ represents the transfer function component at frequency f, describing wave propagation from the position of excitation towards the damage. Then $d(f)$ is an entry that expresses the frequency dependent scattering that occurs when the waves reach the defect. Lastly, $t_s(f)$ introduces the transfer function frequency component for the propagation from the defect towards the sensor. In the following, to retain simplicity, the frequency dependency will be dropped.

Assuming the more general case of m excitations and a single point-scatterer in the medium, the m approximations for the scattered signals are written in a vector notation:

$$\mathbf{SC}_{[m\times 1]} = \mathbf{T}_{\mathbf{e}[m\times 1]} * \mathbf{D}_{[1\times 1]} * \mathbf{T}_{\mathbf{s}[1\times 1]}. \tag{2}$$

Subsequently, expanding to the general case of l point-scatterers, the first and last term on the right-hand side of Equation (2) are substituted with matrices $\mathbf{T}_{\mathbf{E}[m\times l]}$ and $\mathbf{T}_{\mathbf{S}[l\times 1]}$. These matrices describe wave propagation from the excitations towards the defects and propagation from the defects back to the sensor respectively. In addition, the single element matrix $\mathbf{D}$ is also replaced by a diagonal matrix of $[l \times l]$ dimensions. Each element across the diagonal represents the scattering coefficient for a given defect. This leads to the following scattering vector:

$$\mathbf{SC}_{[m\times 1]} = \mathbf{T}_{\mathbf{E}[m\times l]} * \mathbf{D}_{[l\times l]} * \mathbf{T}_{\mathbf{S}[l\times 1]}. \tag{3}$$

2.2 Damage localization

With the previous approximation of the scattered field, it is assumed that the location of damage is known and that the scattering coefficients along with the corresponding transfer functions are available. However it is usually the case that the location and number of defects are unknown and solving the inverse problem is of interest. In such cases, it is possible to generalize the approximation of Equation (3) with a set of unknown but possible defect locations L. Specifically, when replacing the actual l scatterers with the set of the L possible scatterers the parametric Equation (4) arises:

$$\mathbf{SC}_{[m\times 1]} = \mathbf{T}_{\mathbf{E}[m\times L]} * \mathbf{D}_{[L\times L]} * \mathbf{T}_{\mathbf{S}[L\times 1]}. \tag{4}$$

In this case, assuming the diagonal matrix is unknown, solving the system for $\mathbf{D}_{[L\times L]}$ serves as an indication for the damage location and severity. Specifically, zero-values elements across the diagonal imply that the respective damage location, although possible, is not actually contributing in the scattered field. On the other hand, non-zero entries indicate locations of active scattering. As a result, Equation (4) becomes the equivalent of Equation (3) when using zero values for the coefficients that are not actively contributing as damage. Equation (4) is further simplified in the standard linear problem of Equation (5):

$$\mathbf{SC}_{[m\times 1]} = \mathbf{T}_{\mathbf{E}[m\times L]} * \mathbf{x}_{[L\times 1]} \tag{5}$$

In this expression x serves as the unknown parameter whose solution recovers both the location and severity of the damage.

2.3 The exact solution

Considering that for most real-life applications the number of possible defects can be greater than the number of installed sensors and therefore independent measurements, a system such as the one of Equation (5) is often under-determined. In practice this means that there is no exact solution in the damage localization problem. The problem arises from the fact that arbitrary combinations of possible defect locations and scattering coefficients can be used to reconstruct the observed field. An expensive solution for this problem is to install more than L sensors and turn Equation (5) into a well-defined system. Another more moderate approach is to assume that the number of excitations and sensors only exceeds the l actual defects, with $l << L$. Subspacing techniques such as the MUSIC algorithm [22] utilize this approach. Nevertheless they can still require large array installations when l is large or unknown.

2.4 Sparsity approximation

In order to solve the linear problem when only a single sensor is available, additional constraints must be introduced in the system. However, considering that the number of unknown parameters is generally large it becomes infeasible to define appropriate relationships and retrieve an exact solution. As an alternative, physics-based contstraints can be introduced that penalize a larger family of solutions. As discussed, sparsity is such a case. Considering damage is a sparse phenomenon in the medium, when thinking in terms of the underdetermined system, only sparse solutions for x should be recovered. To quantify the level of sparseness the L_0-norm of x can be used. However considering this is not a convex penalty, it is common to approximate it with the L_1-norm. Equation (5) transforms then to the minimization problem of Equation (6), also known as the Lasso formulation [11]:

$$L(\mathbf{x}) = min_{\mathbf{x}} \left\{ \frac{1}{2} \left\| \mathbf{SC} - \mathbf{T_E x} \right\|_2^2 + \lambda \left\| \mathbf{x} \right\|_1 \right\}. \tag{6}$$

Equation (6) can be also seen as a Least Squares regression with an added penalty. In this case the penalty term consists of the L_1-norm of the solution vector scaled by a regularization parameter λ. This parameter dictates the significance of the penalty in the minimization process.

3 Sparsity methods for damage localization

Identifying the importance of sparse constraints, a methodology to solve the undetermined problem is presented in this section. Using complex scattered information as input, this method is able to recover multiple damage positions even when a single sensor setup is available. An adaptive framework of the algorithm is also discussed which aims to enhance the performance in cases of limited detectability.

3.1 The group lasso

In practice, solving Equation (6) requires operating on responses in the frequency domain which are commonly complex-valued. The imaginary part of the data contributes phase information for the signal and is often the result of attenuation phenomena that took place in the structure. Lasso however is not appropriate for operating on such data. The alternative of a separate solution for the real and imaginary components would imply an approximation with no interaction between these terms. To answer this problem, in the literature [23] it is proposed to treat the Lasso problem of complex entries as a Group Lasso of real entries. The Group Lasso is a special formulation of Lasso which other than searching for the sparsest solution also tries to satisfy some inherent structure for the regression. Namely, if the solution vector was separated in two

groups it is possible to require for the j^{th} elements of both groups to be zero-valued. This is a quite useful property when treating complex numbers. If the complex solution vector of dimensions $[L \times 1]$ was to be substituted by a real-valued vector of dimensions $[2L \times 1]$ with the first L entries being the real components while the rest correspond to the imaginary terms, a necessary constraint would impose that both real and imaginary components of the same complex zero-valued coefficient are also zero-valued. The Group Lasso problem formulates then into Equation (7):

$$L(\mathbf{x}) = min_{\mathbf{x}} \left\{ \frac{1}{2} \left\| \begin{bmatrix} \mathbf{SC}_r \\ \mathbf{SC}_i \end{bmatrix} - \begin{bmatrix} \mathbf{T}_{\mathbf{E}r} & -\mathbf{T}_{\mathbf{E}i} \\ \mathbf{T}_{\mathbf{E}i} & \mathbf{T}_{\mathbf{E}r} \end{bmatrix} \begin{bmatrix} \mathbf{x}_r \\ \mathbf{x}_i \end{bmatrix} \right\|_2^2 + \lambda \left\| \mathbf{x} \right\|_1 \right\}, \tag{7}$$

where subscripts r and i denote matrices of real and imaginary components, respectively. In Equation (7), the L_1-norm of complex components can also be written as

$$\left\| \mathbf{x} \right\|_1 = \sum_{i=1}^{l} \left| \mathbf{x}_i \right| = \sum_{i=1}^{l} \sqrt{Re(\mathbf{x}_i)^2 + Im(\mathbf{x}_i)^2} = \sum_{i=1}^{l} \left| \mathbf{x}_i \right|_2 = \left| \tilde{\mathbf{x}} \right|_{2,1}. \tag{8}$$

The l rows of matrix $\tilde{\mathbf{x}}$ are populated with the pairs of real and imaginary components for the different $\mathbf{x}_i$. As a consequence of Equations (7) and (8), the complex minimization problem of Equation (6) formulates into the following real-valued Group Lasso regression:

$$L(\tilde{\mathbf{x}}) = min_{\tilde{\mathbf{x}}} \left\{ \frac{1}{2} \left\| \begin{bmatrix} \mathbf{SC}_r \\ \mathbf{SC}_i \end{bmatrix} - \begin{bmatrix} \mathbf{T}_{\mathbf{E}r} & -\mathbf{T}_{\mathbf{E}i} \\ \mathbf{T}_{\mathbf{E}i} & \mathbf{T}_{\mathbf{E}r} \end{bmatrix} \begin{bmatrix} \mathbf{x}_r \\ \mathbf{x}_i \end{bmatrix} \right\|_2^2 + \lambda \left\| \tilde{\mathbf{x}} \right\|_{2,1} \right\}. \tag{9}$$

3.2 The Adaptive Group Lasso

Zou [12] proposed the adaptive Lasso to enable the oracle properties for Lasso related routines. With this algorithm the authors demonstrated that it possible to consistently identify the correct solutions independently of the regularization parameters. Equation (10) follows this implementation which can be seen as a variation of Equation (6) with independent weights for the different variables:

$$L(\mathbf{x}) = min_{\mathbf{x}} \left\{ \frac{1}{2} \left\| \mathbf{SC} - \mathbf{T}_{\mathbf{E}} \mathbf{x} \right\|_2^2 + \lambda \sum_{j=1}^{L} w_j \left| x_j \right| \right\}. \tag{10}$$

For this algorithm, the weights should behave as an initial estimation for the final solution. This however is not always feasible. In the Adaptive Group Lasso algorithm of [24] an iterative process that selects weights for the regression on a group of frequencies k_i based on the solution from a group of frequencies k_{i-1} is proposed. Using this method allows each of the predefined frequency groups to serve as an initial estimator for subsequent groups until they are all processed. The final result is seen to achieve damage maps of more prominent peaks with respect to the Group Lasso and less noise-sensitive results. This method will be used here to enhance cases that Group Lasso fails to achieve satisfactory localization.

4 Experiments

In this section both methods are evaluated over a series of experiments. Specifically, focus is drawn on their ability to localize multiple defects in the same structure and on their robustness to noisy environments. In the following paragraphs, the setup and the necessary configurations are described for the conducted experiments. During the designed campaigns damage localization is evaluated on a composite panel with simulated and actual defects being induced in the structure. Damage maps depict the recovered degradation zones.

4.1 Setup

Localization is investigated in a 5mm thick, square cross-ply composite plate of 400mm edge length. The first damage case, of simulated scatterers, examines the possibility of multi-defect localization. For this case three added masses are installed on the structure as defects. Masses have been extensively used in literature as a benchmark case that approximates degradation. For the second damage case, of an actual degradation, a permanent defect is induced. For this investigation a slit is selected for its reproducibility. The induced damage has a length of 102mm and width of 4mm. Figures 1a and 1b show both damage configurations on the composite structure. In Figure 1a the position of the masses is given while on Figure 1b the slit is seen. In both figures, the coordinate system used to position the defects, the excitations and the sensor is also presented. Figure 2 demonstrates the selected geometry serving as a point-scatterer. The mass for each of these defects was measured to be 55gr.

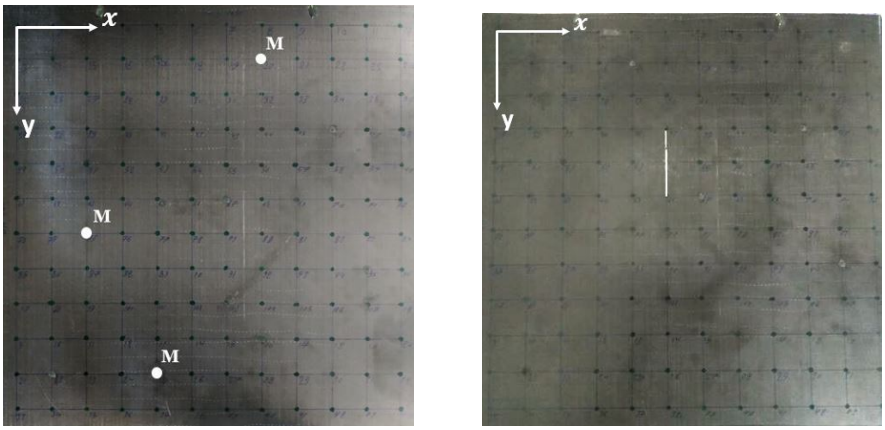

(a) Damage 1: Point-Scatterers (b) Damage 2: Slit

Figure 1: The composite plate with the introduced defects

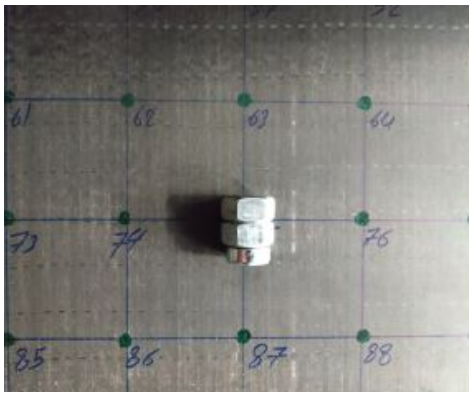

Figure 2: Selected geometry for the added mass damage

4.2 The experiment

To achieve localization both techniques presented in section 3, rely on a system of equations with known inputs and outputs. In an experimental campaign, roving hammer (PCB 086C03) excitations are used. The resulting acceleration fields that constitute the system's output are measured with a 1-D accelerometer (PCB 352a24). Overall a number of broadband acceleration responses are measured on a single sensor. Frequencies up to 1600Hz are studied. For higher values the effect of noise starts to become more prominent and the sensitivity of the sensor is not sufficient to resolve damage information. In addition, averaging across 5 repetitions was applied for every experiment to negate remaining noise effects.

Specifically, for the case of the point-scatterers and the slit damage, 7 and 5 impacts were used respectively. In general, a higher number of excitations is expected to lead to a better resolution for more complex cases. Tables 1 and 2 detail the positions of the impacts and the location of the sensor with respect to the coordinate systems given in Figure 1.

Table 1: Excitations and Sensor coordinates for Damage 1: Point-Scatterers

	E_1	E_2	E_3	E_4	E_5	E_6	E_7	S
Point	17	46	51	67	95	116	122	67
x (mm)	200	450	100	300	500	350	50	300
y (mm)	50	150	200	250	350	450	500	250

Table 2: Excitations and Sensor coordinates for Damage 2: Slit

	E_1	E_2	E_3	E_4	E_5	S
Point	17	46	67	95	122	95
x (mm)	200	450	300	500	50	500
y (mm)	50	150	250	350	500	350

On a first round of measurements the left-hand side of Equation (5) is obtained. Experiments for this process are performed on the healthy and the damaged structure in order to identify the scattered field. On a second round of experiments, the matrix of transfer functions on the right-hand side of Equation (5) is defined. For this, responses on the healthy state have to be measured across a grid of possible damage points. In this case, 144 points are defined, with 7 and 5 responses being measured on each point for the two damage cases respectively. Overall, this step consists of an offline process that is damage-invariant and can be performed once before any damage occurs. In conclusion, $\mathbf{SC}$ and $\mathbf{T_E}$ can now be assembled and the algorithms are enabled for localization.

5 Results

In this section, results for the achieved damage localization are discussed. The Group Lasso algorithm is first validated under the two damage scenarios. Damage maps are presented highlighting the positions of damage. The performance of the algorithm is then discussed as the complexity of the problem arises. For the more challenging cases the adaptive approach is deployed to enhance the obtained detectability. A comparison against the MUSIC reference is also drawn to quantify the effectiveness with respect to a well established algorithm under the same single sensor conditions.

5.1 Group lasso

The Group Lasso technique is used here to perform damage localization for the two defect cases. First its performance is evaluated in the multi-defect case of three point-defects. Figure 3a depicts the damage map obtained from this experiment. As it can be seen, damage signatures of varying resolution have been identified for all three scatterers in the structure. In the damage map, peaks are indicated with lighter colors with respect to the background. Although all defects are visible, at least one of them is not clearly resolved. That is, the corresponding indication does not significantly deviate from the background average. This implies that the Group Lasso approach may find some limitations for cases where numerous scatterers are to be identified and the level of sparsity decreases. In the next section, the adaptive approach discussed in Section 3.2 will also be used to evaluate this case.

On a second investigation, the real damage case of an induced slit was analyzed. The slit, as discussed already, defines a reproducible non point-like damage case. Results shown in Figure 3b demonstrate the obtained damage map for this scatterer. It can be seen that the location of the defect is strongly identified in

the damage map as a sharp peak that significantly deviates from the background average. Hence it becomes clear that the Group Lasso approach is not limited to point-like defects. To explain this behavior we follow the reasoning of Marengo et al. [25] in order to approach an extended defect as a collection of point-sources which if closely located they can be identified as an effective contribution. Therefore it is reasonable to expect for an extended defect to be recovered by means of an equivalent scatterer in that location. In the following sections, the slit experiment will also be used to study the performance of localization under increasing noise levels.

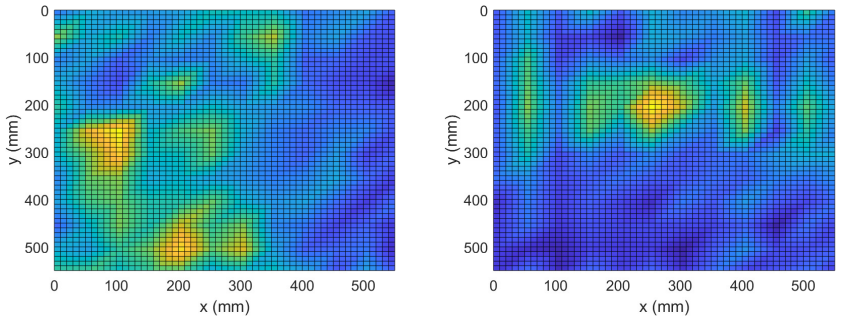

(a) Damage 1: Point-Scatterers (b) Damage 2: Slit

Figure 3: Damage localization with Group Lasso

5.2 Adaptive group lasso for multiple defects

Considering Group Lasso may not be able to resolve all defects, in this section the Adaptive Group Lasso approach with 10 randomly-sampled frequency groups is applied in an attempt to successfully position the scatterers. The damage maps of Figure 4 demonstrate the achieved detection from both techniques. In comparison, the new damage map of Figure 4b is now able to localize all scatterers with greater accuracy. Moreover the lack of false positive indications is also prominent. The enhanced performance of the adaptive approach is further quantified with the bar-chart of Figure 5. In this graph the peak-to-average ratio is drawn on the three damage locations. Namely, for both damage maps, the peak value on every position of known defect is scaled by the global average of the background indication to define a ratio. Comparison is then performed for the given metric on each damage location. Higher values imply significant deviation from the background and possible detection on the position of the scatterer while lower values translate to unresolved peaks.

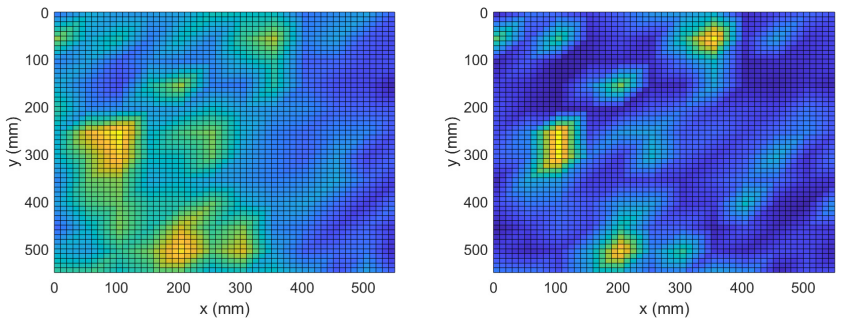

(a) Group Lasso (b) Adaptive Group Lasso

Figure 4: Point-Scatterer localization with Group Lasso and Adaptive Group Lasso

Figure 5 reveals that for every damage position the adaptive methodology is able to resolve the scatterers with peaks at least twice more dominant than the ones achieved with the Group Lasso approach. We can

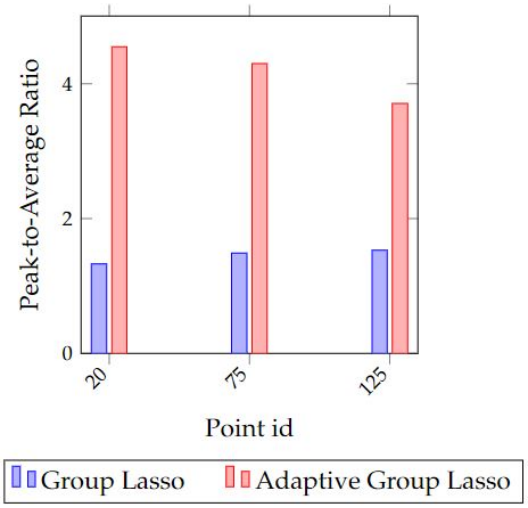

Figure 5: Peak-to-average ratio for the point-scatterers case with Group Lasso and Adaptive Group Lasso

therefore identify that for multi-defect scenarios the Adaptive Group Lasso is the preferred approach.

5.3 Adaptive group lasso for noisy signals

In this section, the effect of noise on localization is investigated. To this end, starting from the successful positioning with the Group Lasso technique on the slit case, localization will be evaluated under multiple noise levels. Specifically, noise of uniform distribution is added on the observed damage fields to simulate three levels of Signal to Noise Ratio (SNR). Hence, SNR values of 35dB, 25dB and 15dB are assumed. Figure 6 depicts the three damage maps obtained from the respective cases. As it can be seen, for high and moderate values of SNR the performance of Group Lasso does not significantly deteriorate from the reference as discussed in Section 5.1. However for extremely noisy environments such as for SNR of 15dB, the ability to localize the defect is lost. Only a faint indication is present which cannot reliably be attributed to damage. On the other hand, when this scenario is processed with the adaptive approach damage detection is possible. That is observed with Figure 7 where for the case of 15dB SNR damage maps are plotted and it is seen that the Adaptive Group Lasso is able to magnify the otherwise faint indication of the Group Lasso approach. It can be thus concluded that other than the multi-scatterer scenario, Adaptive Group Lasso is also suitable for high noise environments.

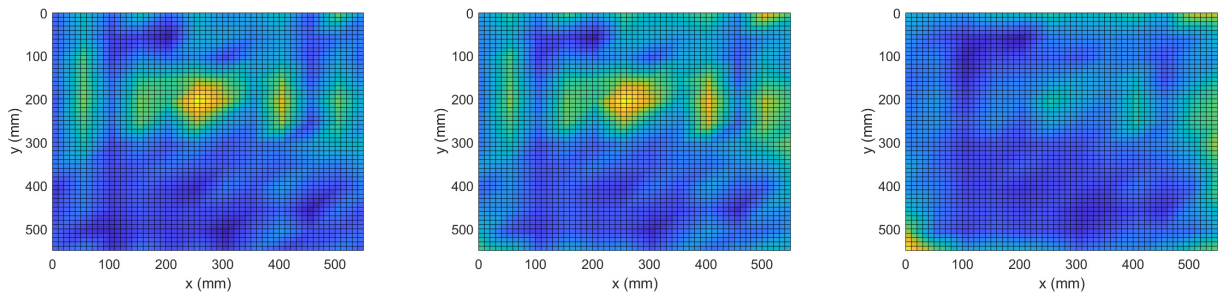

(a) SNR: 35dB (b) SNR: 25dB (c) SNR: 15dB

Figure 6: Slit localization with Group Lasso and varying SNR

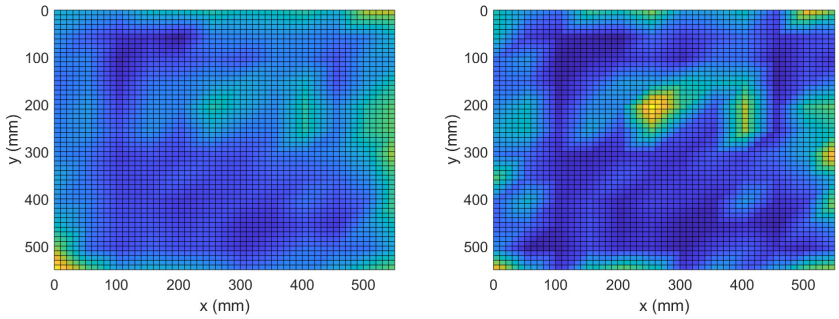

(a) Group Lasso (b) Adaptive Group Lasso

Figure 7: Slit localization with Group Lasso and Adaptive Group Lasso with SNR of 15dB

5.4 Comparisons with MUSIC

Having evaluated the performance of both techniques under the multi-defect scenario and the presence of noise, it is also important to extract conclusions on their performance against similar but competitive techniques. As discussed, one of these methods would be the Multiple Signal Classification (MUSIC) algorithm. In contrast to Lasso, MUSIC is a fully deterministic approach that relies on signal decomposition and a large array of sensors to localize damage. Under these conditions MUSIC has been seen to be able to resolve multiple scatterers for a range of environments and applications [26, 27, 28, 29]. However the need for large sensor arrays is one of MUSIC's important shortcomings. Specifically, for a case of l scatterers, MUSIC would require at least an array of l sensors. Once these conditions are satisfied, the algorithm resolves sufficient independent information to establish a complete basis for the signal under decomposition. In turn this allows localization of extreme accuracy, also known as the super-resolution property. Nevertheless, the requirement of large sensor arrays, is in general considerably expensive for the arbitrary detection problem. Therefore in the following MUSIC will be used to localize defects on both damage cases using the same reduced arrays as the ones given in Tables 1 and 2.

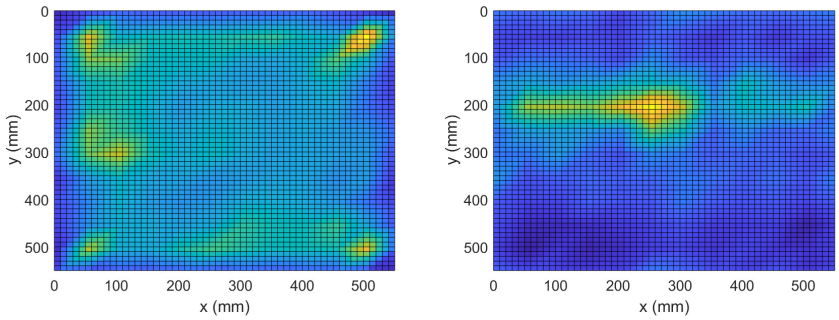

(a) Damage 1: Point-Scatterers (b) Damage 2: Slit

Figure 8: Single sensor damage localization with MUSIC

Figure 8 shows the obtained damage maps for both cases of the multiple scatterers and the induced slit. As it can be seen, MUSIC fails to localize the large number of scatterers using a single sensor. On the other hand, in Figure 8b the damage map is clearly able to localize the slit with an accuracy competitive to that of Group Lasso. Although this may seem counter-intuitive it is still an expected behavior considering the fact that a single extended damage can be approximated as an equivalent point-scatterer in the region [25]. Hence, it should be expected that MUSIC will be able to localize that defect with a single sensor array. As a result it can be concluded that for single damage cases the Group Lasso methodologies approximate the behavior of the single sensor MUSIC as the probabilistic and deterministic paths intersect. On the other hand, under the multi-scatterer scenario, the single sensor MUSIC is not able to localize any of the defects while both Group

Lasso techniques are able to identify important damage signatures.

6 Conclusions

The Group Lasso and the Adaptive Group Lasso methodologies have been studied for the localization of defects using frequency domain complex responses. By exploiting knowledge for the implied sparsity of the damage detection problem, both techniques are able to localize multiple defects with a single-sensor setup. Specifically, the Group Lasso algorithm introduces a sparsity constraint in an otherwise underdetermined problem of grouped signal components to localize damage. The Adaptive Group Lasso manages to further enhance resolution, by accounting for the predictive power of a given frequency-dependent solution when it is used as the initial estimator for a different frequency range. Both algorithms were validated with a number of experimental campaigns. The localization of three added masses on a composite plate was first analysed. It was found that both techniques managed to identify a damage signature for every scatterer. However, the adaptive approach achieved greater resolution with sharper peaks on the corresponding damage map and it is therefore preferred for such scenarios. In addition an extended scatterer in the form of a slit was also evaluated. In that case the defect was successfully localized with both techniques. In particular, for noisy environments, the adaptive approach was seen to amplify the otherwise weak peak the Group Lasso approach resolved. In the last section of this paper, a direct comparison was performed with respect to the established super-resolution technique of MUSIC. There it was seen that although MUSIC is able to localize the slit almost as well as the Group Lasso, it completely fails to resolve the multi-defect scenario of three scatterers. The latter revealed an important limitation of MUSIC and a significant advantage of the sparsity-based techniques.

Acknowledgements

Internal Funds KU Leuven are gratefully acknowledged for their support.

References

[1] F. Magalhães, A. Cunha, and E. Caetano, "Vibration based structural health monitoring of an arch bridge: From automated oma to damage detection," *Mechanical Systems and Signal Processing*, vol. 28, p. 212 – 228, 2012.

[2] J.-T. Kim and N. Stubbs, "Improved damage identification method based on modal information," *Journal of Sound and Vibration*, vol. 252, no. 2, p. 223 – 238, 2002.

[3] A. Pandey and M. Biswas, "Damage detection in structures using changes in flexibility," *Journal of Sound and Vibration*, vol. 169, no. 1, p. 3 – 17, 1994.

[4] J. Cai, L. Shi, S. Yuan, and Z. Shao, "High spatial resolution imaging for structural health monitoring based on virtual time reversal," *Smart Materials and Structures*, vol. 20, no. 5, 2011.

[5] S. Dixon, S. Burrows, B. Dutton, and Y. Fan, "Detection of cracks in metal sheets using pulsed laser generated ultrasound and emat detection," *Ultrasonics*, vol. 51, no. 1, pp. 7–16, 2011.

[6] S. Kessler, S. Spearing, and C. Soutis, "Damage detection in composite materials using lamb wave methods," *Smart Materials and Structures*, vol. 11, no. 2, pp. 269–278, 2002.

[7] B. Glišić and D. Inaudi, *Fibre Optic Methods for Structural Health Monitoring*, 2007.

[8] L. Scalise, Y. Yu, G. Giuliani, G. Plantier, and T. Bosch, "Self-mixing laser diode velocimetry: application to vibration and velocity measurement," *IEEE Transactions on Instrumentation and Measurement*, vol. 53, no. 1, pp. 223–232, 2004.

[9] P. Castellini, M. Martarelli, and E. Tomasini, "Laser doppler vibrometry: Development of advanced solutions answering to technology's needs," *Mechanical Systems and Signal Processing*, vol. 20, no. 6, p. 1265 – 1285, 2006.

[10] H. L. Harter, "The method of least squares and some alternatives. Part I, II, II, IV, V, VI." *International Satistical Review*, vol. 42,43, 1974-1976.

[11] R. Tibshirani, "Regression Shrinkage and Selection Via the Lasso," *Journal of the Royal Statistical Society: Series B (Methodological)*, vol. 58, no. 1, pp. 267–288, jan 1996.

[12] H. Zou, "The adaptive lasso and its oracle properties," *Journal of the American Statistical Association*, vol. 101, no. 476, pp. 1418–1429, dec 2006.

[13] M. Yuan and Y. Lin, "Model selection and estimation in regression with grouped variables," *Journal of the Royal Statistical Society. Series B: Statistical Methodology*, vol. 68, no. 1, pp. 49–67, feb 2006.

[14] C. B. Smith and E. M. Hernandez, "Exploiting Spatial Sparsity in Vibration-based Damage Detection," *Procedia Engineering*, vol. 199, pp. 1925–1930, jan 2017.

[15] X.-Q. Zhou, Y. Xia, and S. Weng, "L1 regularization approach to structural damage detection using frequency data," *Structural Health Monitoring*, vol. 14, no. 6, pp. 571–582, 2015.

[16] A. Entezami, H. Shariatmadar, and H. Sarmadi, "Structural damage detection by a new iterative regularization method and an improved sensitivity function," *Journal of Sound and Vibration*, vol. 399, pp. 285–307, 2017.

[17] D. Sen, A. Aghazadeh, A. Mousavi, S. Nagarajaiah, and R. Baraniuk, "Sparsity-based approaches for damage detection in plates," *Mechanical Systems and Signal Processing*, vol. 117, pp. 333–346, 2019.

[18] Y. Yang and S. Nagarajaiah, "Structural damage identification via a combination of blind feature extraction and sparse representation classification," *Mechanical Systems and Signal Processing*, vol. 45, no. 1, pp. 1–23, 2014.

[19] C. Xu, Z. Yang, S. Tian, and X. Chen, "Lamb wave inspection for composite laminates using a combined method of sparse reconstruction and delay-and-sum," *Composite Structures*, vol. 223, 2019.

[20] Z. Sharif Khodaei and M. Aliabadi, "Assessment of delay-and-sum algorithms for damage detection in aluminium and composite plates," *Smart Materials and Structures*, vol. 23, 07 2014.

[21] O. Mesnil and M. Ruzzene, "Sparse wavefield reconstruction and source detection using compressed sensing," *Ultrasonics*, vol. 67, pp. 94–104, 2016.

[22] R. Schmidt, "Multiple emitter location and signal parameter estimation," *IEEE Transactions on Antennas and Propagation*, vol. 34, no. 3, pp. 276–280, 1986.

[23] M. Carlin, P. Rocca, G. Oliveri, F. Viani, and A. Massa, "Directions-of-arrival estimation through bayesian compressive sensing strategies," *IEEE Transactions on Antennas and Propagation*, vol. 61, no. 7, pp. 3828–3838, 2013.

[24] V. Dimopoulos, W. Desmet, and E. Deckers, "Sparse damage detection with complex group lasso and adaptive complex group lasso," *Sensors*, vol. 22, no. 8, 2022.

[25] E. A. Marengo, F. K. Gruber, and F. Simonetti, "Time-reversal MUSIC imaging of extended targets," *IEEE Transactions on Image Processing*, vol. 16, no. 8, pp. 1967–1984, 2007.

[26] J. He and F. G. Yuan, "Lamb waves based fast subwavelength imaging using a DORT-MUSIC algorithm," *AIP Conference Proceedings*, vol. 1706, no. 2016, 2016.

[27] Y. Zhong, S. Yuan, and L. Qiu, "Multiple damages detection on aircraft composite structures using near-field MUSIC algorithm," *Sensors and Actuators A: Physical*, vol. 214, pp. 234–244, 2014.

[28] R. A. Osornio-Rios, J. P. Amezquita-Sanchez, R. J. Romero-Troncoso, and A. Garcia-Perez, "Music-ann analysis for locating structural damages in a truss-type structure by means of vibrations," *Computer-Aided Civil and Infrastructure Engineering*, vol. 27, no. 9, pp. 687–698, 2012.

[29] H. Zuo, Z. Yang, C. Xu, S. Tian, and X. Chen, "Damage identification for plate-like structures using ultrasonic guided wave based on improved music method," *Composite Structures*, vol. 203, pp. 164–171, 2018.